Nuclear Inst. and Methods in Physics Research B 482 (2020) 25–30

Contents lists available at ScienceDirect

Nuclear Inst. and Methods in Physics Research B

journal homepage: www.elsevier.com/locate/nimb

The comparison of theoretical model calculations and experimental data of ^{58,60,61,64}Ni, ^{64,66,68}Zn, and ^{63,65}Cu photo-nuclear reactions

G.H. Hovhannisyan[a,*], T.M. Bakhshiyan[b], A.S. Danagulyan[a], R.K. Dallakyan[c]

[a] Yerevan State University, 0025, Armenia
[b] Armenian National Agrarian University, Yerevan 0025, Armenia
[c] A. Alikhanyan National Science Laboratory, Yerevan 0036, Armenia

ARTICLE INFO

Keywords:
(γ,n) reaction
GDR region
Talys 1.95
Gamma ray strength function
^{58606164}Ni
^{6365}Cu
^{646668}Zn

ABSTRACT

Photonuclear reactions cross-sections using TALYS 1.95 code in the GDR region were studied to test the reliability of various models of gamma ray strength functions. Six different gamma ray strength function models have been applied. The photo-neutron reactions for the isotopes ^{58,60,61,64}Ni, ^{63,65}Cu, and ^{64,66,68}Zn were investigated. The theoretical results were compared with the experimental data from the EXFOR data library. A relative variance analysis has performed to choose the gamma strength function mode which describes the experimental data the best.

1. Introduction

The study of the properties of the atomic nucleus started at the moment of its discovery and is still a topic of a vast interest. During the years, an extensive experimental database describing the nuclear properties has been accumulated [1], and various theoretical models have been suggested [2] to describe the nuclear properties to various degrees of accuracy. The use in modern astrophysics, nuclear engineering, nuclear medicine, etc. stimulates the rapid development of various models which are able to explain and predict the results of nuclear reactions involving various nuclei and initiated by various particles with a high level of accuracy.

The interaction of the gamma-quantum with atomic nuclei has some unique characteristics. In particular, the reaction cross section has a wide maximum called Giant Dipole Resonance (GDR). The position of the maximum depends on the atomic number and is in the range of 10–30 MeV. The width of the peak is between 4 and 15 MeV [3].

Various theories attempt to explain GDR with the use of different concepts. In the phenomenological theory of the liquid drop model, GDR is modeled as a collective excitation of a large number of nucleons, and can be described by oscillations of two incompressible, mutually penetrating liquids of protons and neutrons [4,5]. The accumulation of nuclear data resulted in a need for new models that take into account the dependence of the width of GDR on the deformation of the nucleus [6,7]. Later, a dynamic, collective model to describe the deformations of the nucleus was proposed that took into account the collective rotational and vibrational degrees of freedom of the surface of the nucleus [8].

At the microscopic level, the motion of the nucleons can be described within the Mean Field Approximation. The resulting energy levels form nuclear shells which are similar to electronic shells in an atom. Within this model, GDR results from transitions between different shells [9]. In an improved model, exchange interactions are also considered, which are not taken into account in the mean field approximation [10]. This modification doesn't destroy the nuclear shell structure, but the energy eigenstates are coherent states in this case, each of which corresponds to a single degree of freedom of the nucleus. For light nuclei that have partially filled outer shells, GDR corresponds to excitations of many independent degrees of freedom corresponding to transitions from different shells [11].

Despite the existence of various theoretical models describing GDR, a single model which accurately describes GDR for all nuclei doesn't exist. As a reason, a number of popular software packages (such as TALYS [12]) include various modifications of phenomenological as well as microscopic models. TALYS is widely used nowadays by various authors for nuclear reaction calculations with different projectiles [13–18]. In this work, we have calculated photonuclear reaction cross-sections using TALYS 1.95 in the energy region of the giant dipole resonance to test the reliability of various models of gamma ray strength functions. We study the dependence of cross sections of photonuclear

* Corresponding author.
E-mail address: hov_gohar@ysu.am (G.H. Hovhannisyan).

https://doi.org/10.1016/j.nimb.2020.09.001
Received 10 August 2020; Received in revised form 28 August 2020; Accepted 2 September 2020

reactions of ^{58,60,61,64}Ni, ^{63,65}Cu, and ^{64,66,68}Zn target isotopes on the choice of strength functions. ^{68}Zn is of interest because of its applications in the production of the medical radioisotope ^{67}Cu, and our calculations serve as a preliminary estimation for ^{67}Cu production planning. Reactions on ^{63,65}Cu are often used to monitor flux estimation and to calculate flux-weighted average cross-sections in experiments with bremsstrahlung [19–21]. ^{58,60,62,64}Ni isotopes were chosen because of having a magic proton number which results in an extensive experimental data of nuclear reactions involving Ni isotopes; this allows a more precise calculation of accuracy of TALYS calculations in the considered nuclear mass range.

2. Calculation methods

For nuclear reaction simulations various input parameters are needed, such as nuclear masses, characteristics of the ground and excited states of the nucleus, level densities, optical potentials, GDR parameters and so on. For calculations using software packages such as ALICE, EMPIRE, GNASH, UNF, TALYS, these parameters are taken from the RIPL-3 (Reference Input Parameter Library) database [22].

When modelling nuclear reactions which include transitions between excited levels, the concept of the gamma-ray strength function, which is related to the photoabsorption cross section, is often introduced. In the phenomenological approach, various modifications of the Lorentzian are used to describe the strength function. However, for most unstable nuclei there aren't enough data points to fit the phenomenological model parameters of GDR, and therefore this description is impossible. Because of this, various microscopic models are of use, and are included in nuclear reaction parameter calculation software systems such as TALYS.

TALYS 1.9 includes 8 different models of gamma-ray strength functions [12]. In this article we discuss 5 of these that describe the experiment better.

The first two of the models described in this article use a Lorentzian representation of the GDR: Kopecky-Uhl model uses a Generalized Lorentzian form (Modified Lorentzian model, MLO), and Brink-Axel model uses a Standard Lorentzian (Standard Lorentzian model, SLO). In SLO giant dipole resonance shape is described by [12]:

$$f_{Xl}(E_\gamma) = K_{Xl}\frac{\sigma_{Xl}E_\gamma\Gamma_{Xl}^2}{(E_\gamma^2 - E_{Xl}^2) + E_\gamma^2\Gamma_{Xl}^2} \quad (1)$$

where σ_{Xl}, $E_\gamma$and Γ_{Xl} are the strength, energy and the width of GDR, respectively, and $K_{Xl} = \frac{1}{(2l+1)\pi^2\hbar^2c^2}$.

In MLO, the GDR shape is described by [12]:

$$f_{E1}(E_\gamma, T) = K_{E1}\left[\frac{E_\gamma\widetilde{\Gamma}_{E1}(E_\gamma)}{(E_\gamma^2 - E_{E1}^2)^2 + E_\gamma^2\widetilde{\Gamma}_{E1}(E_\gamma)^2} + \frac{0.7\Gamma_{E1}4\pi^2T^2}{E_{E1}^3}\right]\sigma_{E1}\Gamma_{E1} \quad (2)$$

where $\widetilde{\Gamma}_{E1}(E_\gamma) = \Gamma_{E1}\frac{E_\gamma^2 + 4\pi^2T^2}{E_{E1}^2}$ is the energy dependent damping width, and $T = \sqrt{\frac{E_n + S_n - \Delta - E_\gamma}{a(S_n)}}$ (where S_n is the neutron separation energy, E_n is the incident neutron energy, Δ the pairing correction, and a is the level density parameter at S_n).

Two other models are based on the microscopic theories - Hartree-Fock BCS tables (HF), Hartree-Fock-Bogolyubov tables (HFB) [22] - which contain the tabulated microscopic gamma ray strength functions, calculated from the corresponding theory for each isotope.

The fifth model is Goriely's hybrid model (GHM) which has a Lorentzian form but also includes the effects of the pygmy resonance [23].

The latest version of TALYS package (version 1.95) introduced some updates to gamma-ray strength functions. In particular, E1 data tables were improved, Simplified Modified Lorentzian (SMLO) was introduced [24]. Calculations using SMLO model are also included in the article.

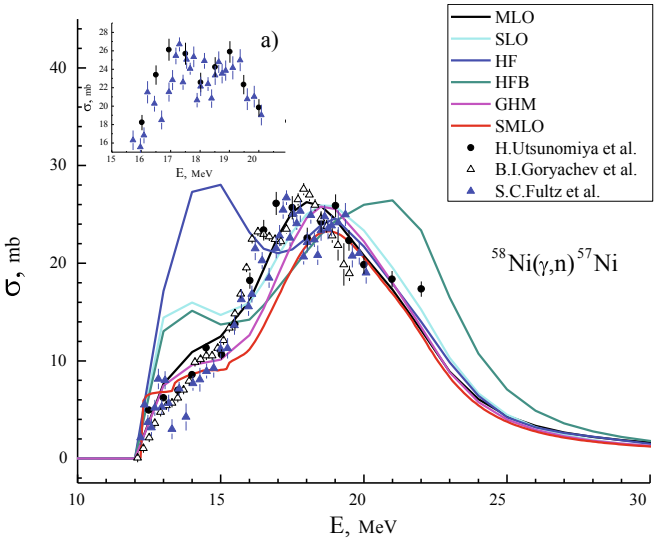

Fig. 1. ^{58}Ni(γ,n)^{57}Ni reaction cross-section.

3. Results and discussion

The cross sections of ^{58}Ni(γ,n)^{57}Ni, ^{60}Ni(γ,n)^{59}Ni, ^{61}Ni(γ,n)^{60}Ni, ^{64}Ni(γ,n)^{63}Ni, ^{63}Cu(γ,n)^{62}Cu, ^{63}Cu(γ,2n)^{61}Cu, ^{65}Cu(γ,n)^{64}Cu, ^{64}Zn (γ,n)^{63}Zn, ^{66}Zn(γ,n)^{65}Zn, and ^{68}Zn(γ,n) ^{67}Zn reactions were simulated using different gamma-ray strength functions of TALYS 1.95. Experimental data from Experimental Nuclear Reaction Data Library (EXFOR) is used to compare the results of the calculations to the experiment [1]

^{61,64}Ni(γ,n) reactions cross-sections have been measured experimentally by Utsunomiya et al. [25], while ^{58,60}Ni(γ,n) reactions were measured by Utsunomiya et al. [25], Goryachev et al. [26], and Fults et al. [27]. The sources of irradiation in the experiments were Laser Compton Scattered Photons, Bremsstrahlung, and Positron annihilations, respectively. All three experimental results were compared to calculations (in case of [26,27] only the data at energies below (γ, pn) reaction threshold were used).

^{58}Ni(γ,n)^{57}Ni reaction data of [25,27] display two humps around the top of the giant dipole resonance (Fig. 1a). Data of [26] are scattered and indicate a complicated structure of GDR (Fig. 1). Gamma-ray strength function models MLO and GHM give similar results and are in a relatively good agreement with the experimental data but do not display the two humps. SMLO results have a similar form to MLO and GHM but are located lower. The HF model displays two humps in the giant dipole resonance region, but the width of GDR is significantly broader. SLO and HFB display small humps in the energy region below 15 MeV, which do not coincide with the experimental data. The maximum of the cross section is shifted towards higher energies in case of HFB which is a recurring result also present in the following calculations using HFB.

^{60}Ni(γ,n)^{59}Ni reaction cross-sections are given in Fig. 2. For this reaction, MLO, SLO, GHM give similar results but the maximum is shifted slightly to lower energies relative to the experiment. The maximum of the distribution is shifted significantly to the lower energies for HF and to the higher energies for HFB.

^{61,64}Ni(γ,n) reactions cross sections were measured by [25] up to energies 19 and 16 MeV, respectively. SMLO, SLO, MLO and GHM give relatively similar results and are close to the experimental ones in the region where the experimental data is available. HF results are significantly wider than all other models for energies below 15–16 MeV. Even though there is no experimental data for higher energies to compare the models to, there is a good agreement between the models in this region (Figs. 3,4).

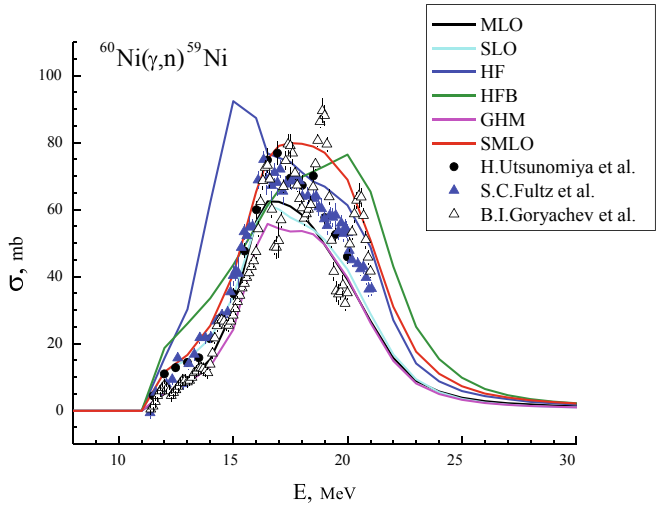

Fig. 2. ^{60}Ni(γ,n)^{59}Ni reaction cross-section.

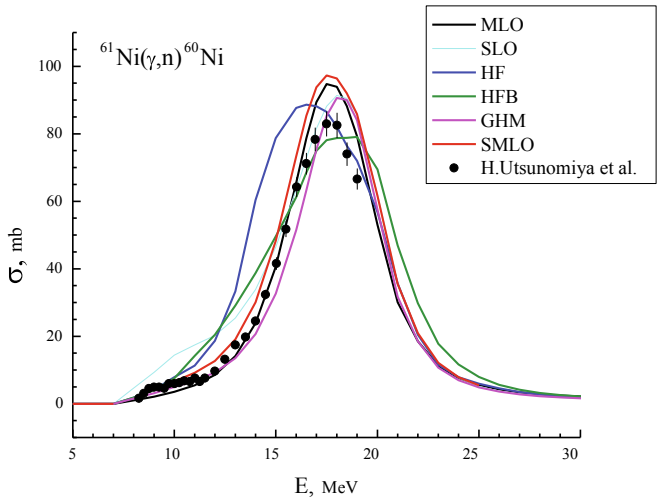

Fig. 3. ^{61}Ni(γ,n)^{60}Ni reaction cross-section.

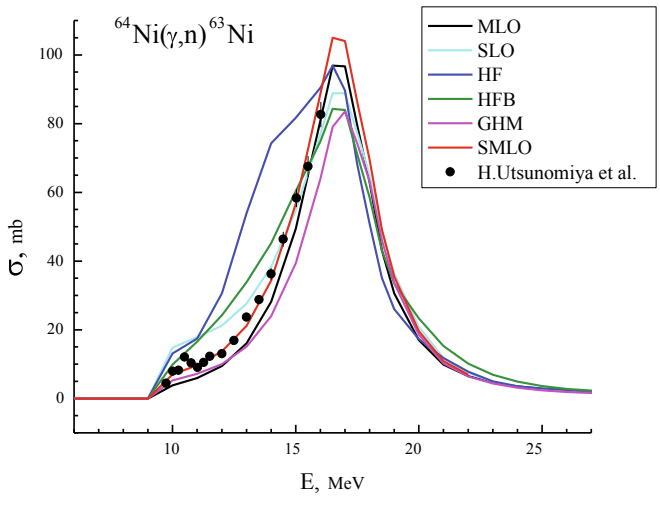

Fig. 4. ^{64}Ni(γ,n)^{63}Ni reaction cross-section.

The quality of the description of available experimental data with the TALYS 1.95 code was estimated based on statistical analysis. We determine the relative variance of theoretical and experimental data, D, using [28]:

Table 1
Relative variance of theoretical and experimental data for Ni isotopes.

Autors	Models					
	MLO	SLO	HF	HFB	GHM	SMLO
^{58}Ni(γ,n)^{57}Ni						
Utsunomiya et al.	0.1473	0.4230	0.7478	0.4332	0.1705	0.1783
Goryachev et al.	0.3534	0.871672	1.2451	0.8198	0.3997	0.3953
Fultz et al.	0.2731	0.6658	1.0372	0.6084	0.2721	0.2597
Average	**0.2579**	**0.6534**	**1.0100**	**0.6205**	**0.2808**	**0.2777**
^{60}Ni(γ,n)^{59}Ni						
Utsunomiya et al.	0.2180	0.1744	0.7469	0.4809	0.2751	0.2341
Fultz et al.	0.1935	0.1821	0.6243	0.3605	0.2581	0.2179
Goryachev et al.	0.2572	0.6541	1.5830	1.3002	0.2965	0.8005
Average	**0.2229**	**0.3369**	**0.9847**	**0.7139**	**0.2766**	**0.4175**
^{61}Ni(γ,n)^{60}Ni						
Utsunomiya et al.	**0.2029**	**0.7572**	**0.5330**	**0.4335**	**0.1525**	**0.2009**
^{64}Ni(γ,n)^{63}Ni						
Utsunomiya et al.	**0.3053**	**0.5077**	**0.8456**	**0.4213**	**0.2932**	**0.0967**

$$D = \left\{ \frac{1}{N} \sum_{i=1}^{N} |\sigma_i^{calc} - \sigma_i^{exp}| / \sigma_i^{exp} \right\} \quad (3)$$

where σ_i^{calc} is the calculated cross section, σ_i^{exp} is the experimental cross section, and N is the number of experimental data points. The results are presented in Table 1. According to Relative Variance Analysis (RVA), the best strength function model for ^{58,60}Ni(γ,n) reaction is MLO, for ^{61}Ni(γ,n) – GHM, and for ^{64}Ni(γ,n) – MSLO. These three models result in similar values of D for all Ni isotopes and are better fits to the experimental data than the other three models (see Table 1).

In Figs. 5–7 we present cross section calculations for ^{63}Cu and ^{65}Cu together with the same cross sections measured using quasi-monochromatic γ-rays produced by an annihilation of monoenergetic positrons [29–31]. In case of reference [29] only data up to the (γ,pn) reaction threshold were used. The MLO model, display similar results (Fig. 5) for ^{63}Cu(γ,n)^{62}Cu reaction, and the calculated data follow the shape of the experimental results but are shifted to the lower energies. HF and HFB give a good description of the data for energies higher than 20 MeV. SLMO gives the most accurate description of the experimental data in this case (see Table 2 and Fig. 5).

In the case of ^{65}Cu(γ,n) ^{64}Cu + ^{65}Cu(γ,np) ^{63}Ni reaction, MLO, SLO and GHM results are again similar and fit the experimental measurements quite well (Fig. 7). The calculations of HF and HFB lay higher for the whole spectrum. SMLO results are in between the two. The best strength function model for ^{65}Cu(γ,n) ^{64}Cu + ^{65}Cu(γ,np)^{63}N reaction according to RVA is GHM (see Table 2).

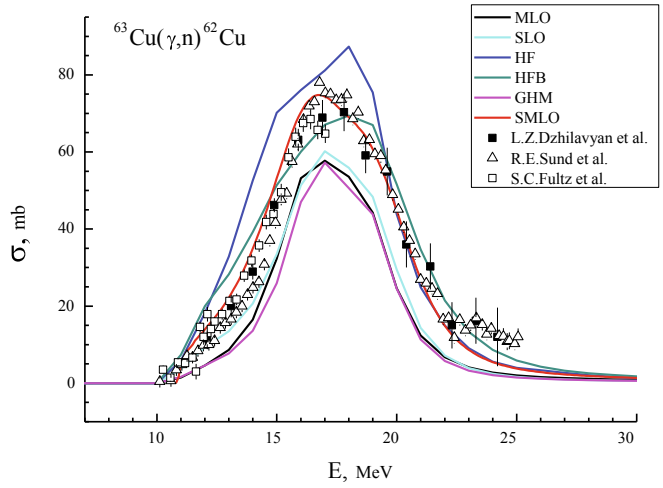

Fig. 5. ^{63}Cu(γ,n)^{62}Cu reaction cross-section.

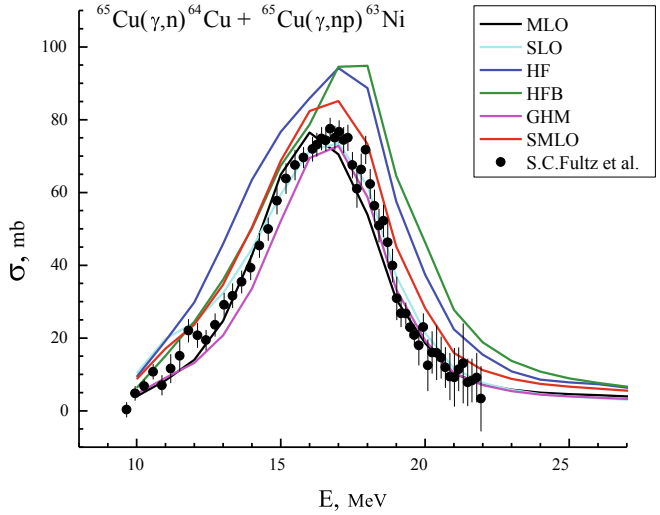

Fig. 6. $^{65}Cu(\gamma,n)^{64}Cu$ + $^{65}Cu(\gamma,np)^{63}Ni$ reaction cross-section.

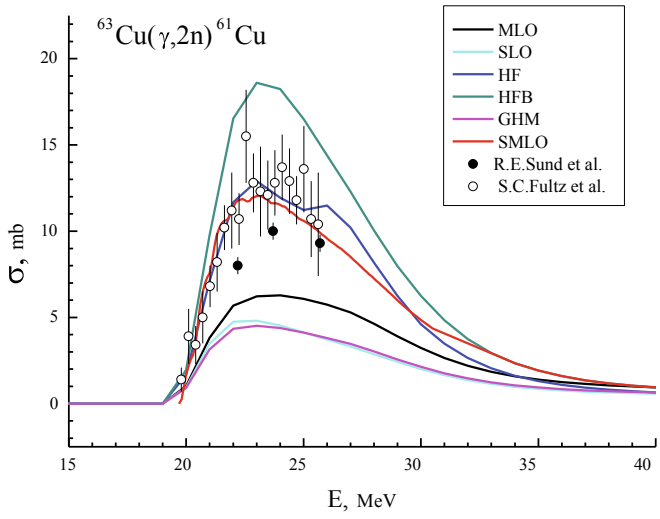

Fig. 7. $^{63}Cu(\gamma,2n)^{61}Cu$ reaction cross-section.

Table 2
Relative variance of theoretical and experimental data for Cu isotopes.

Autors	Models					
	MLO	SLO	HF	HFB	GHM	SMLO
$^{63}Cu(\gamma,n)^{62}Cu$						
Dzhilavyan et al.	0.4556	0.3737	0.3862	0.2346	0.5038	0.1951
Sund et al.	0.4936	0.3953	0.4807	0.3680	0.5397	0.2884
Fultz et al.	0.5027	0.4066	0.6302	0.5635	0.5410	0.3372
Average	***0.4840***	***0.3919***	***0.4991***	***0.3887***	***0.5311***	***0.2735***
$^{65}Cu(\gamma,n)^{64}Cu$ + $^{65}Cu(\gamma,np)^{63}Ni$						
Fultz et al.	**0.2811**	**0.3251**	**0.9230**	**1.0202**	**0.2578**	**0.4141**
$^{63}Cu(\gamma,2n)^{61}Cu$						
Sund et al.	0.3362	0.5075	0.3299	0.8744	0.5281	0.2333
Fultz et al.	0.5131	0.6083	0.1427	0.4435	0.6321	0.1641
Average	**0.4247**	**0.5579**	**0.2363**	**0.6589**	**0.5801**	**0.1987**

The SLMO is the best strength function model (Fig. 7 and Table 2) for $^{63}Cu(\gamma,2n)61Cu$ reaction, which is often used as a monitor for photons flux estimation [19–21].

$^{64,66,68}Zn(\gamma,n)$ reactions cross–section calculations with gamma-ray strength functions are given in Figs. 8–10. We used quasi-monochromatic γ-ray source data of [32] and bremsstrahlung source data of [33,34] for comparison of the calculated results with the experiment. In case of Ref. [33] only the data at energies below (γ, pn) reaction threshold were used.

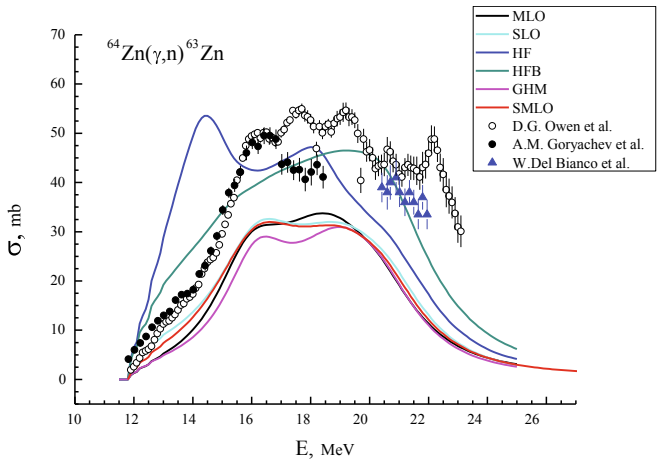

Fig. 8. $^{64}Zn(\gamma,n)^{63}Zn$ reaction cross-section.

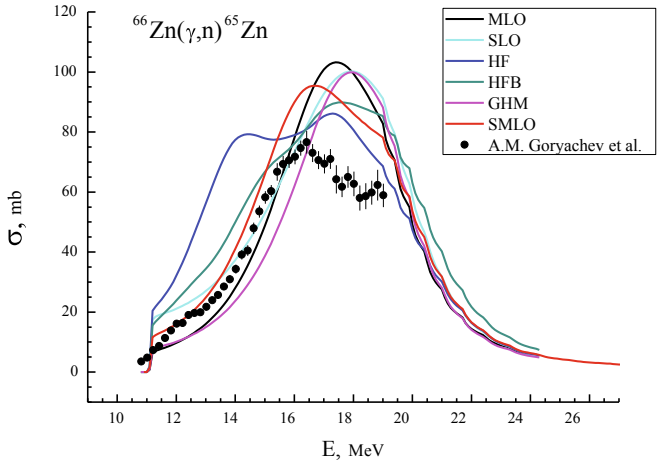

Fig. 9. $^{66}Zn(\gamma,n)^{65}Zn$ reaction cross-section.

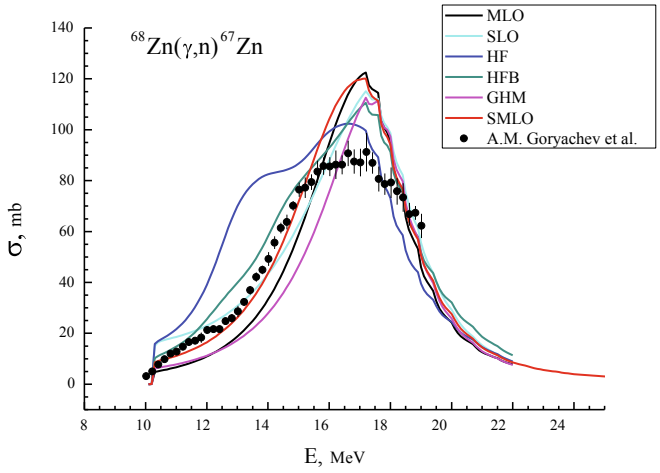

Fig. 10. $^{68}Zn(\gamma,n)^{67}Zn$ reaction cross-section.

The results from MLO, SLO, GHM, and SLMO models for $^{64}Zn(\gamma,n)^{63}Zn$ reaction are close to each other, but lay lower for the entire spectrum. HF and HFB results are very different from the other models: they are situated higher and are noticeably wider, which results in a better fit to the experiment. HFB is the best description of the reaction

Table 3
Relative variance of theoretical and experimental data for Zn isotopes.

Autors	Models					
	MLO	SLO	HF	HFB	GHM	SMLO
^{64}Zn(γ,n)^{63}Zn						
D.J. Owen et al.	0.4721	0.3792	0.6482	0.3292	0.5142	0.4219
A.M. Goryachev et al.	0.4148	0.3261	0.5111	0.2085	0.4767	0.3695
W. Del Bianco et al.	0.5306	0.4698	0.3473	0.1217	0.5299	0.5010
Average	**0.4148**	**0.3261**	**0.5111**	**0.2085**	**0.4767**	**0.4608**
^{66}Zn(γ,n)^{65}Zn						
A.M. Goryachev et al.	**0.3294**	**0.3646**	**0.6949**	**0.4260**	**0.3596**	**0.2761**
^{68}Zn(γ,n)^{67}Zn						
A.M. Goryachev et al.	**0.3338**	**0.2384**	**0.5458**	**0.2197**	**0.3346**	**0.2043**

according to RVA (see Table 3 and Fig. 8).

In the case of ^{66}Zn(γ,n)^{66}Zn and ^{68}Zn(γ,n)^{67}Zn reactions all models give similar results for energies higher than 19 MeV. SMLO is the best fit to the experimental data (see Table 3).

4. Conclusions

Photo-neutron reaction cross-sections of ^{58}Ni(γ,n)^{57}Ni, ^{60}Ni(γ,n)^{59}Ni, ^{61}Ni(γ,n)^{60}Ni, ^{64}Ni(γ,n)^{63}Ni, ^{63}Cu(γ,n)^{62}Cu, ^{63}Cu(γ,2n)^{61}Cu, ^{65}Cu(γ,n)^{64}Cu, ^{64}Zn(γ,n)^{63}Zn, ^{66}Zn(γ,n)^{65}Zn, and ^{68}Zn(γ,n)^{67}Zn reactions have been investigated using different gamma-ray strength function models included in TALYS 1.95. A single model of gamma-ray strength function that works the best for all reactions considered couldn't be identified. In the majority of considered cases, the phenomenological models give better descriptions of the observed data. HF model has been the least successful (with the sole exception of ^{63}Cu(γ,2n)^{61}Cu reaction) when comparing the calculations with the experimental results based on the absolute value as well as based on the shape of GDR. The SMLO model, only included in the latest TALYS version 1.95, is the only one describing ^{63}Cu cross sections accurately and can be used for flux estimation and to calculate flux-weighted average cross-sections in experiments with bremsstrahlung. For photo-neutron reactions on ^{65}Cu, GHM is the best gamma-ray strength function model. Moreover, the MLO, GHM, and SLMO give similar results on photo-neutron reactions for Ni nuclei and are the best models to describe the experimental data. MLO is the best model for ^{58,60}Ni isotopes, GHM - for ^{61}Ni, and SMLO - for ^{64}Ni. In case of ^{64}Zn(γ,n)^{63}Zn reaction, the MLO, SLO, GHM, and SLMO models give similar results and describe the shape of GDR well, but are located lower for the entire spectrum. For ^{66,68}Zn isotopes, calculated data are higher than the experimental ones on the maximum. A reevaluation of the parameters used is needed in this case.

CRediT authorship contribution statement

G.H. Hovhannisyan: Conceptualization, Methodology, Writing - review & editing. **T.M. Bakhshiyan:** Software, Data curation, Investigation. **A.S. Danagulyan:** Supervision. **R.K. Dallakyan:** Software, Validation, Formal analysis.

Declaration of Competing Interest

The authors declare that they have no known competing financial interests or personal relationships that could have appeared to influence the work reported in this paper.

Acknowledgements

This work was made possible in part by a research grant from the Yervant Terzian Armenian National Science and Education Fund (ANSEF) based in New York, USA.

References

[1] https://www-nds.iaea.org/exfor/.
[2] A. Kamal, pp 353–423 Nuclear Models, Nuclear Physics. Graduate Texts in Physics, Springer, Berlin, Heidelberg, 2014, , https://doi.org/10.1007/978-3-642-38655-8_6.
[3] B.L. Berman, Atlas of photoneutron cross sections obtained with monoenergetic photons, At. Data Nucl. Data Tables 15 (1975) 319, https://doi.org/10.1016/0092-640X(88)90033-2.
[4] M. Goldhaber, E. Teller, On nuclear dipole vibrations, Phys. Rev. 74 (1948) 1046, https://doi.org/10.1103/PhysRev.74.1046.
[5] A. Migdal, Quadrupole and dipole γ-radiation of nuclei, J. Phys. Acad. Sci. USSR 8 (1–6) (1944) 331.
[6] M. Danos, On the long-range correlation model of the photonuclear effect, Nucl. Phys. 5 (1958) 23, https://doi.org/10.1016/0029-5582(58)90005-1.
[7] K. Okamoto, Intrinsic quadrupole moment and the resonance width of photonuclear reactions, Phys. Rev. 110 (1958) 143, https://doi.org/10.1103/PhysRev.110.143.
[8] M. Danos, W. Greiner, Dynamic theory of the nuclear collective model, Phys. Rev. 134 (1964) B284, https://doi.org/10.1103/PhysRev.134.B284.
[9] D. Wilkinson, Nuclear photodisintegration, Physica 22 (1956) 1039, https://doi.org/10.1016/S0031-8914(56)90061-1.
[10] G.E. Brown, M. Bolstrely, Dipole state in nuclei, Phys. Rev. Lett. 3 (1959) 472, https://doi.org/10.1103/PhysRevLett.3.472.
[11] R.A. Eramzhyan, B.S. Ishkhanov, I.M. Kapitonov, V.G. Neudatchin, The giant dipole resonance in light nuclei and related phenomena, Phys. Rep. 136 (1986) 229, https://doi.org/10.1016/0370-1573(86)90136-5.
[12] A. Koning, S. Hilaire and S. Goriely "TALYS 1.9. A nuclear reaction program" December 21, 2017. http://www.talys.eu/.
[13] E. Vagena, S. Stoulos, Average cross section measurement for ^{162}Er (γ, n) reaction compared with theoretical calculations using TALYS, Nucl. Phys. A 957 (2017) 259, https://doi.org/10.1016/j.nuclphysa.2016.09.007.
[14] S. Stoulos, E. Vagena, Indirect measurement of bremsstrahlung photons and photoneutrons cross sections of ^{204}Pb and Sb isotopes compared with TALYS simulations, Nucl. Phys. A 980 (2018) 1, https://doi.org/10.1016/j.nuclphysa.2018.09.081.
[15] H. Naik, G. Kim, M. Zaman, et al., Photo-neutron reaction cross-sections of ^{59}Co in the bremsstrahlung end-point energies of 65 and 75 MeV, Eur. Phys. J. A 55 (2019) 217, https://doi.org/10.1140/epja/i2019-12915-y.
[16] H. Naik, S.V. Suryanarayana, M.S. Murali, et al., Excitation function of ^{68}Zn(p, n)^{68}Ga reaction for the production of ^{68}Ga, J Radioanal Nucl. Chem. 324 (2020) 285, https://doi.org/10.1007/s10967-020-07037-4.
[17] G.H. Hovhannisyan, A.S. Danagulyan, T.M. Bakhshiyan, ^{96g}Tc as an alternative gamma-ray emitter for medical diagnostics, Phys. Atom. Nucl. 82 (1) (2019) 1, https://doi.org/10.1134/S1063778819010101.
[18] P.V. Cuong, T.D. Thiep, L.T. Anh, et al., Theoretical calculation by Talys code in combination with Geant4 simulation for consideration of reactions of Eu isotopes in the giant dipole resonance region, Nucl. Instr. Meth. B 479 (2020) 68, https://doi.org/10.1016/j.nimb.2020.06.011.
[19] A.S. Danagulyan, G.H. Hovhannisyan, T.M. Bakhshyan, et al., Formation of medical radioisotopes ^{111}In, $^{117\ m}$Sn, ^{124}Sb, and ^{177}Lu in photonuclear reactions, Phys. Atom. Nucl. 78 (2015) 447, https://doi.org/10.1134/S1063778815030035.
[20] T.D. Thiep, T.T. An, N.T. Khai, et al., Determination of the total bremsstrahlung photon flux from electron accelerators by simultaneous activation of two monitors, Phys. Part. Nuc. Lett. 9 (2012) 648, https://doi.org/10.1134/S1547477112080092.
[21] S.S. Belyshev, D.M. Filipescu, I. Gheoghe, et al., Multinucleon photonuclear reactions on 209Bi: Experiment and evaluation, Eur. Phys. J. A 51 (2015) 67, https://doi.org/10.1140/epja/i2015-15067-2.
[22] https://www-nds.iaea.org/RIPL-3/.
[23] S. Goriely, Radiative neutron captures by neutron-rich nuclei and the r-process nucleosynthesis, Phys. Lett. B 436 (1998) 10, https://doi.org/10.1016/S0370-2693(98)00907-1.
[24] A. Koning, S. Hilaire, S. Goriely, TALYS 1.95. A nuclear reaction program" December 24, 2019.
[25] H. Utsunomiya, T. Renstrom, G.M. Tveten, et al., Photoneutron cross sections for Ni isotopes: Toward understanding (n, γ) cross sections relevant to weak s-process nucleosynthesis, Phys. Rev. C 98 (2018) 054619, , https://doi.org/10.1103/PhysRevC.98.054619.
[26] B.I. Goryachev, B.S. Ishkhanov, I.M. Kaptono, I.M. Piskarev, V.G. Shevchenko, O.P. Shevchenko, Sov. J. Nucl. Phys. 11 (1970) 141.
[27] S.C. Fultz, R.A. Alvarez, B.L. Berman, P. Meyer, Photoneutron cross sections of ^{58}Ni and ^{60}Ni, Phys. Rev. C 10 (1974) 608, https://doi.org/10.1103/PhysRevC.10.608.
[28] N.V. Kurenkov, V.P. Lunev, Y. Shubin, Evaluation of calculation methods for

excitation functions for production of radioisotopes of iodine, thallium and other elements, App. Rad. Isot. 50 (1999) 541, https://doi.org/10.1016/S0969-8043(98)00048-7.
[29] S.C. Fultz, R.L. Bramblett, J.T. Caldwell, R.R. Harvey, Photoneutron cross sections for natural Cu, ^{63}Cu and ^{65}Cu, Phys. Rev. 133 (1964) B1149, https://doi.org/10.1103/PhysRev.133.B1149.
[30] R.E. Sund, M.P. Baker, L.A. Kull, R.B. Walton, Measurements of the ^{63}Cu(gamma, n) and (gamma,2n) cross sections, Phys. Rev. 176 (1968) 1366, https://doi.org/10.1103/PhysRev.176.1366.
[31] L.Z. Dzhilavyan, N.P. Kucher, Study of the cross section of the reaction Cu-63(gamma, n) on the beam of quasimonochromatic annihilation photons in energy range 12–25 MeV, Yad. Fiz. 30 (1979) 294.
[32] W. Del Bianco, S. Kundu, P. Boucher, ^{64}Zn(gamma,n)^{63}Zn cross section from 20.4 to 21.9 MeV, Can. J. Phys. 5 (1973) 1302.
[33] A.M. Goryachev, G.N. Zalesnyy, The studying of the photoneutron reactions cross sections in the region of the giant dipole resonance in zinc, germanium, selenium, and strontium isotopes, Voprosy Teoreticheskoy i Yadernoy Fiziki 1982 (8) (1982) 121.
[34] D.G. Owen, E.G. Muirhead, B.M. Spicer, Structure in the giant resonance of ^{64}Zn and ^{63}Cu, Nucl. Phys. A 122 (1968) 177, https://doi.org/10.1016/0375-9474(68)90711-2.